

SF₆/Ar plasma textured periodic glass surface morphologies with high transmittance and haze ratio of ITO:Zr films for amorphous silicon thin film solar cells



Shahzada Qamar Hussain^{a, c}, Gi Duk Kwon^a, Shihyun Ahn^b, Sunbo Kim^a, Hyeongsik Park^b, Anh Huy Tuan Le^b, Chonghoon Shin^a, Sangho Kim^a, Shahbaz Khan^a, Jayapal Raja^b, Nagarajan Balaji^a, S. Velumani^{b, d}, Didier Pribat^a, Junsin Yi^{a, b, *}

^a Department of Energy Science, Sungkyunkwan University, Suwon, 440-746, Republic of Korea

^b College of Information and Communication Engineering, Sungkyunkwan University, Suwon, 440-746, Republic of Korea

^c Department of Physics, COMSATS Institute of Information Technology, Lahore, 54000, Pakistan

^d Department of Electrical Engineering (SEES), CINVESTAV-IPN, 2508, Avenida IPN, Col San Pedro Zacatenco, Mexico City, CP 07360, Mexico

ARTICLE INFO

Article history:

Received 20 October 2014

Received in revised form

28 March 2015

Accepted 1 April 2015

Available online 12 April 2015

Keywords:

ITO:Zr films

SF₆/Ar plasma

rms roughness

Haze ratio

Modulated surface morphology

Amorphous silicon thin film solar cell

ABSTRACT

We report various SF₆/Ar plasma textured periodic glass surface morphologies with high transmittance, haze ratio, and root mean square (rms) roughness of ITO:Zr films for amorphous silicon thin film solar cells (a-Si TFSCs). SF₆/Ar plasma textured glass surface morphologies contain micro- and nano-textured features that help to scatter the light in visible and near infra-red (NIR) wavelength regions. We designed the textured glass surface morphologies with big square craters to smaller pyramids for various glass etching times from 30 to 75 min. Magnetron sputtered ITO:Zr (~210 nm) films were deposited on textured glass surface morphologies and showed higher transmittance and haze ratio of 88.48% and 77.61%, respectively, in the visible-NIR (400–1100 nm) wavelength region. The sheet resistance and resistivity of ITO:Zr films decreased with the increase of etching time, due to high rms roughness and better step coverage. A passivation AZO (30 nm) layer was added to the ITO:Zr films, due to its better stability against hydrogen plasma exposure. The ITO:Zr/AZO films were employed as a front TCO layer and the current density–voltage (J–V) characteristics of a-Si TFSCs increased by light scattering effect, without any reduction in either the open circuit voltage (V_{oc}) or the fill factor (FF). Relative to flat glass substrate, J_{sc} and the efficiency of a-Si TFSCs were enhanced by 7.51% and 19.39%, respectively, for textured glass surface morphology.

© 2015 Elsevier Ltd. All rights reserved.

1. Introduction

Amorphous silicon thin film solar cells (a-Si TFSCs) are considered as promising candidates for future high efficiency large-area and low cost photovoltaic devices. The performance of a-Si TFSCs can be improved by minimizing the optical and electrical losses. The optical losses can be reduced by employing a thinner transparent conductive oxide (TCO) layer, as a substitute for the randomly textured fluorine doped tin oxide (FTO) and aluminum

doped zinc oxide (AZO) films textured with approximately 1 μm thickness [1–3]. Light trapping allows a reduction of reflection losses with an increase in the optical path length of incident light, as well as reductions in the size and material cost of the photovoltaic devices. Randomly textured wet and dry etched glass surface morphologies with high rms roughness and haze ratio are proposed for high efficiency a-Si TFSCs [4–8]. Recently, the periodic textured surfaces received a great deal of interest, due to their ability for high current density compared to randomly textured surface morphologies. The size and cost of photovoltaics can be reduced by employing periodic boundary conditions in optical calculations and uniformity in textured surface morphologies [5,9]. Textured glass surface morphologies also reduced the electrical and optical losses compared to textured TCO films. Uniformly deposited TCO films with high rms roughness and haze ratio can scatter more

* Corresponding author. College of Information and Communication Engineering, Sungkyunkwan University, Suwon, 440-746, Republic of Korea. Tel.: +82 31 290 7139; fax: +82 31 290 7159.

E-mail address: yi@yurim.skku.ac.kr (J. Yi).

light, reduce the overall size of the device, and improve the performance of a-Si TFSCs.

For solar cell applications, the surface morphology of glass can mainly be modified by wet chemical and dry etching processes. Even though wet chemical etching is simple and inexpensive, it is difficult when trying to control the glass surface morphology. The inductive coupled plasma-reactive ion etching (ICP-RIE) process has received much attention, as the glass surface can be textured with high rms roughness and haze ratio. Hongsingthong et al. [6–8] reported the influence of ICP-RIE textured glass substrates with high rms roughness and haze ratio of ZnO films for high efficiency a-Si TFSCs, due to their nano- and micro-size textured surface morphologies. Isabella et al. [4] reported the concept of modulated surface morphologies with various geometrical features for an enhanced scattering mechanism. These nano- and micro-size textured surface morphologies can scatter the light in the visible and NIR wavelength regions [4,7–10]. Jantong et al. reported the influence of ZnO:B films deposited on W textured low cost soda lime glass surface morphologies, with high haze ratio and low reflectance for TFSCs [11]. The influence of various textured glass surface morphologies on the performance of TFSCs has been reported in a few simulation studies [12–14]. Battaglia et al. reported a comparative study of random and periodic surface morphologies for a-Si TFSCs [15]. Recently, Hussain et al. [37] reported the uniform 3D hydrothermally deposited zinc oxide (ZnO) nanorods with high haze ratio for the a-Si TFSCs. We previously reported the light trapping mechanism in periodic textured glass substrates for high haze ratio of ITO films [5]. Various suitable future periodic textured glass surface morphologies for a-Si TFSCs are shown in Fig. 1. The main aim is to replace the commercial FTO glass by periodic textured glass with enhanced performance. These periodic SF₆/Ar plasma textured glass surface morphologies showed better light scattering with high current density due to micro- and nano-size textured features. This alternative approach can enhance the performance and lower down the cost of a-Si TFSCs fabrication. Even though various reports have been presented related to the textured glass surface morphologies for the a-Si TFSCs, the influence of periodic front textured glass surface morphologies for the high transmittance and haze ratio, and low sheet resistance of ITO:Zr films in a-Si TFSCs has yet to be reported.

We report the SF₆/Ar plasma textured periodic glass surface morphologies for high transmittance and haze ratio of ITO:Zr films for a-Si TFSCs. Various surface morphologies of textured glass and ITO:Zr films as a function of glass etching time are discussed. The optical transmittance and haze ratio of ITO:Zr films as a function of glass etching time is explained. The rms roughness, sheet resistance, and electrical characteristics of ITO:Zr films deposited on the textured glass surface morphologies are also discussed. Finally, the influence of textured glass surface morphologies on the performance of a-Si TFSCs is discussed.

2. Experimental details

We present the SF₆/Ar plasma texturing of Corning (Eagle, 2000) glass substrates for various surface morphologies using an ICP-RIE system. The glass substrates were cleaned using acetone, methanol, and distilled water for 15 min each in an ultrasonic bath, followed by blowing with N₂ gas. The annealing was performed at 100 °C for 10 min to vaporize the remaining moisture on the glass surface. The thermal evaporation system was used to deposit Al (~800 nm) on the glass surface. A uniform positive photo-resist (PR) (AZ-7220) layer was deposited on the Al surface of glass by spin-coating, followed by soft baking for 10 min at 120 °C. The square-size patterns with the dimension of (8 × 4) μm² were transferred onto the PR by ultra-violet (UV) photo-lithography. The hard baking was performed for 15 min at 140 °C, followed by Al etching and PR removal. An optical microscope (OM) system was used to verify the pattern formation.

An ICP-RIE (ATS CVD series Etcher-200) system with a load-lock chamber was used for the SF₆/Ar plasma texturing of glass substrates. RF, biased power, and SF₆/Ar flow rates were kept constant at 650 W, 200 W, and 50/50 sccm, respectively, while etching time was varied from 30 to 75 min at regular intervals. The glass substrates (2.5 × 2.5) cm² were attached to a 4 inch Si wafer placed on a wafer chuck. The rear side temperature of the wafer chuck was maintained at 18 °C by circulating the cooling water through a chiller. ITO:Zr films with uniform thickness of ~200 nm were deposited by a RF magnetron sputtering system, using an ITO:Zr target composed of 90 wt% of In₂O₃, 9.8 wt% of SnO₂, and 0.2 wt% of ZrO₂, with 99.999% purity. The passivation AZO (~30 nm) layer was

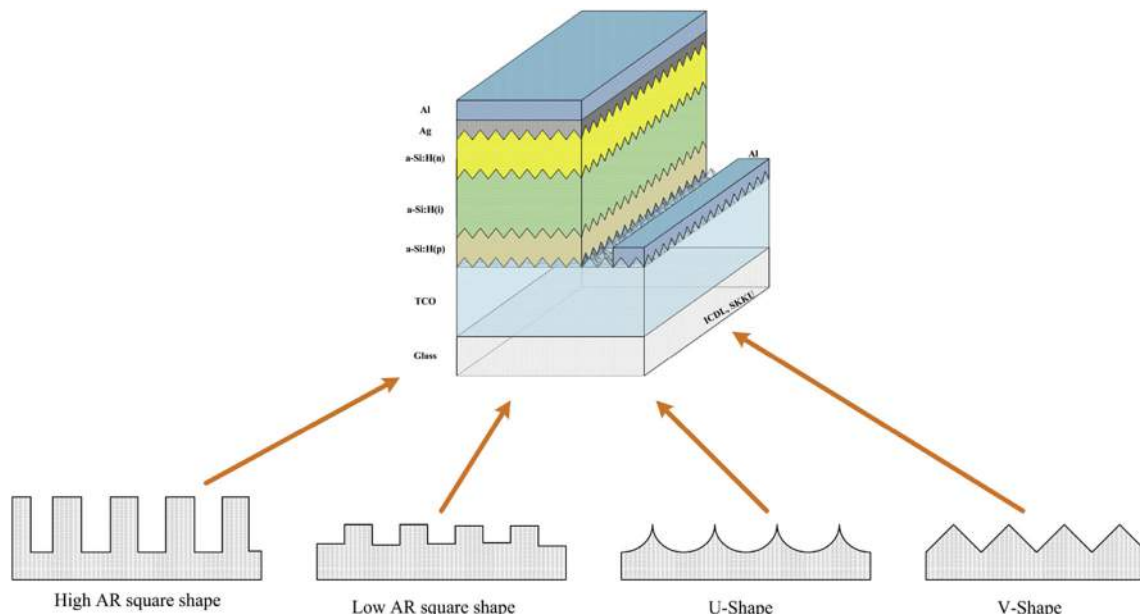


Fig. 1. Schematic diagram of various textured glass surface morphologies in a-Si thin film solar cells.

added to the ITO:Zr layer due to its good stability against hydrogen plasma exposure. The base and working pressure of the sputtering system were maintained at 1×10^{-5} and 2×10^{-3} Torr, respectively. To observe the influence of textured glass surface morphologies, p-i-n a-Si:H TFSCs were deposited on ITO:Zr/AZO films using a cluster type plasma enhanced chemical vapor deposition (PECVD) system. After the deposition of the a-Si (p, i, n) layers, the Ag and Al metal electrodes were deposited using a thermal evaporation method. Fig. 1 shows the complete a-Si TFSC device structure, and various types of future periodic glass surface morphologies.

The surface morphology and etching rates of the periodic textured glass substrates were measured using scanning electron microscopy (SEM Hitachi S-4800). A 3-D alpha step profiler (Dektak XT) system was used to measure the rms roughness and 3-D surface morphologies of ITO:Zr films deposited on the textured glass. The optical characteristics (total, diffused transmittance) were measured using the solar cell spectral response (QE/IPCE QEX7) measurement system. The sheet resistances of the ITO:Zr and ITO:Zr/AZO films were measured using a four probe (CMT-series) system. A Hall effect measurement (Ecopia HMS-3000) system with 1 mA current and magnetic field of 0.51 T was used to measure the

electrical properties of resistivity (ρ) carrier concentration (n), and Hall mobility (μ) of ITO:Zr and ITO:Zr/AZO films. The performance of a-Si TFSCs was measured from current density-voltage (J-V) measurements, under the air mass of 1.5 (100 mW/cm^2) at room temperature.

3. Results and discussion

Fig. 2(a)–2(d) shows the surface morphologies (cross-sectional view) of the SF_6/Ar plasma textured glass substrates for various etching times. The shape of the surface morphology of the textured glass changed from a low depth square to a pyramid, with the increase in etching time from 30 to 75 min. The under-cut of the Al hard mask was mainly related to chemical etching and micro-trenching, which increase with time. Ar was added to SF_6 gas to minimize the under-cut and micro trench formation caused by the rapid removal of by-products [16–18]. A maximum etching depth of $\sim 4.09 \mu\text{m}$ was recorded for the etching time of 75 min Fig. 2(e) shows the etching rate of SF_6/Ar plasma textured glass as a function of etching time. A minor decrease in the etching rate was seen from 58.66 to 54.53 nm/min, with the increase in etching time from

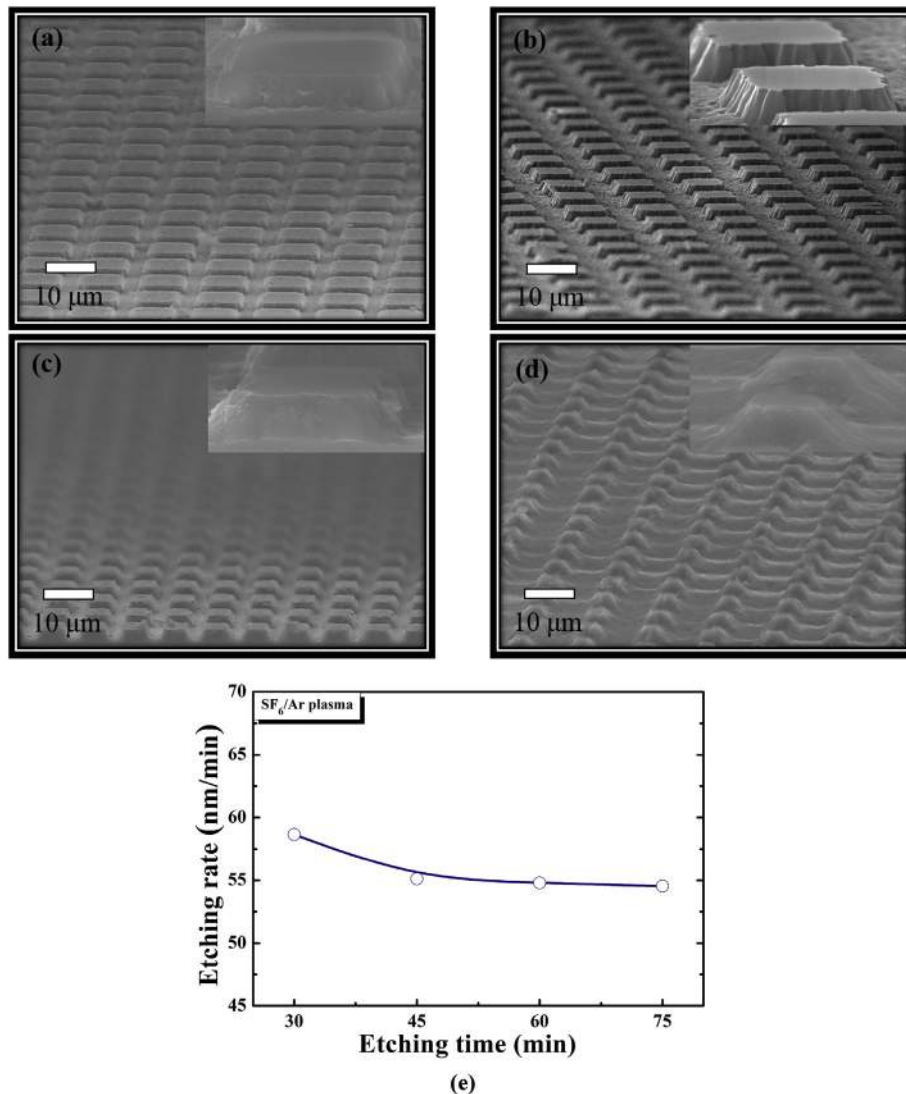


Fig. 2. SEM images of SF_6/Ar plasma textured glass substrates for various etching times, (a) 30 min, (b) 45 min, (c) 60 min, (d) 75 min; and (e) the etching rate of textured glass surface morphologies.

30 to 75 min since, with the increase of etching time, more by-products were produced that lowered the etching rate. On the other hand, the lower etching rates of textured glass were due to the presence of higher percentages of metal elements, such as Ca, B, Al, and Na. These metal elements produced non-volatile etched products, after reacting with halogen gases. Ar gas helps to remove these non-volatile etched products by physical etching [5,16–18].

Fig. 3 shows the surface morphologies of ITO:Zr film deposited on the SF₆/Ar plasma textured glass substrates for various etching times. Recently, ITO:Zr films with high transmittance and work function have been proposed for future high performance photovoltaic applications [19–23,36]. ITO:Zr films deposited on square to pyramid shaped SF₆/Ar plasma textured glass surface morphologies for etching time from 30 min to 75 min. It was reported previously that the rms roughness of TCO films increases with an increase in the etching time. Fig. 3(a)–3(d) shows the micro-size textured surfaces, while Fig. 3(e) shows the nano-size textured surface morphology of ITO:Zr films. The surface morphologies of TCO films played a vital role in improving the step coverage, and hence the sheet resistance. An ideal TCO surface morphology has not yet been defined, but the pyramid shaped textured surface morphology showed good step coverage, high rms roughness, and low sheet resistance [7,11,24,25,28].

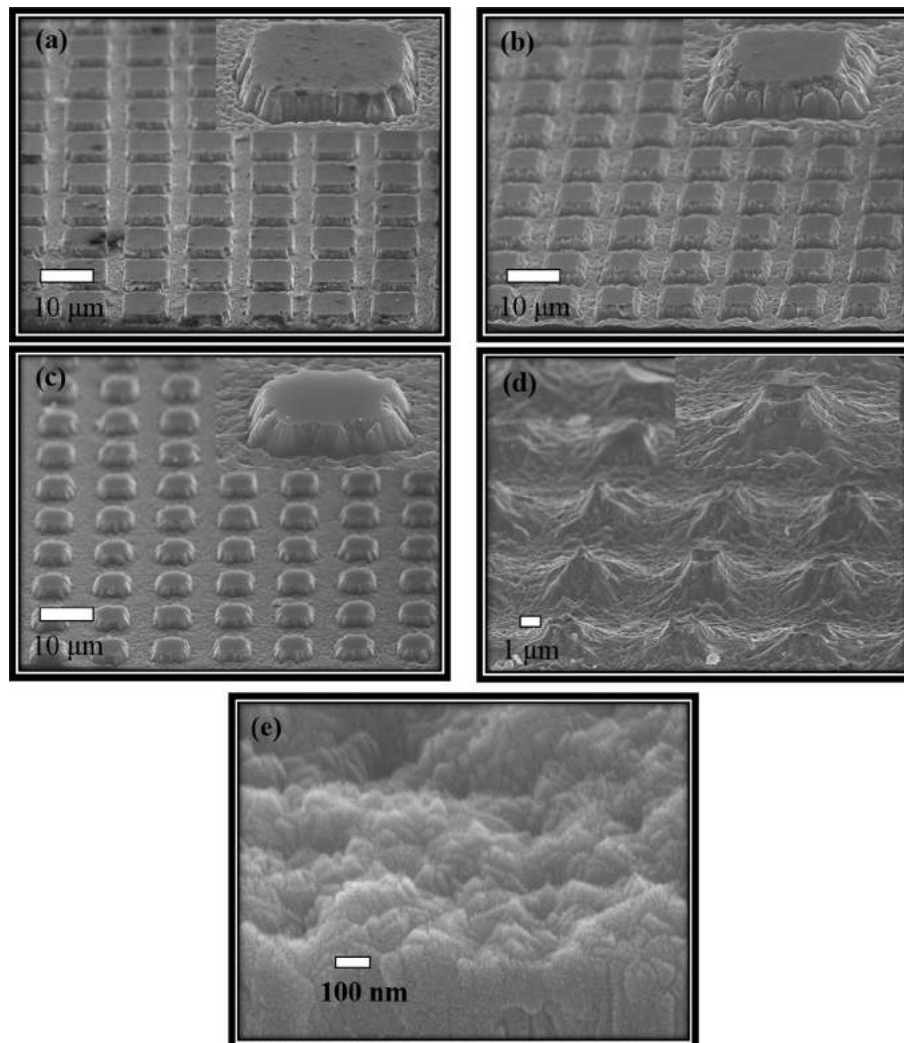


Fig. 3. SEM images of ITO:Zr films deposited on SF₆/Ar plasma textured glass surface morphologies, for various etching times, of (a) 30 min, (b) 45 min, (c) 60 min, (d) 75 min, and the (e) nano-size textured surface morphology of ITO:Zr films taken from the non-periodic side.

Fig. 4 shows the 3-D alpha step profiler images of ITO:Zr films deposited on textured glass surface morphologies as a function of etching time. The (100 × 100) μm² surface area was scanned, to observe the 3-D surface morphology and roughness of the ITO:Zr film. The rms roughness of ITO:Zr films for the glass etching time of 30 min was shown to be 92 nm. The rms roughness of ITO:Zr films increased from 205 nm to 461 nm, with an increase of etching time from 45 to 75 min, respectively. The 3-D surface morphology of ITO:Zr films changed from a low aspect ratio square shape to a V pyramid shape, with an increase of etching time from 30 to 75 min Fig. 4(e) shows the profile height of the ITO:Zr film surface morphologies for various etching times. The profile height showed good agreement with the 3-D profiler images of the ITO:Zr surface morphologies [23,24,26].

The total transmittance of the ITO:Zr films deposited on the textured glass substrates for various etching times is shown in Fig. 5. Total transmittance of the ITO:Zr films was characterized by inserting an index matching fluid Diiodomethane (CH₂I₂, n = 1.74) to suppress the optical reflection losses at the textured glass/ITO:Zr interface [7,25–27]. As-deposited ITO:Zr films showed an average transmittance of 90.82% in the visible-NIR wavelength (400–1100) nm region. The total transmittance of ITO:Zr films increased from 88.03% to 88.48%, as the glass etching time

increased from 30 to 45 min. With further increase in glass etching time from 45 to 75 min, the total visible-NIR transmittance of the ITO:Zr films decreased to 85.55%. It can be seen from the above transmittance data that the surface morphology of glass substrates has a minor influence on the total transmittance of the ITO:Zr films. All the ITO:Zr films showed a total transmittance of above 85% in the visible-NIR wavelength (400–1100) nm region. The haze ratio of the ITO:Zr films is shown in Fig. 5(b) as a function of the glass etching time. The as-deposited ITO:Zr films showed a haze ratio of 0.79% in the visible wavelength region. As the glass etching time increased from 30 to 75 min, the haze ratio of the ITO:Zr films increased from 43.35% to 73.50% in the visible wavelength. The ITO:Zr films with a glass etching time of 75 min also showed the highest haze ratio of 77.61% in the Vis-NIR wavelength region. Due to the micro- and nano-size textured features of glass surface morphologies, the light can be scattered in visible as well as in NIR wavelength regions, as reported in

various studies [4,10,23,28]. The increase in haze ratio was obviously due to a higher rms roughness, and the modulated surface morphology of ITO:Zr films [6–8,37,38].

Fig. 6(a) shows the sheet resistance of ITO:Zr and ITO:Zr/AZO films deposited on SF₆/Ar plasma textured glass surface morphologies for various etching times. A thin AZO (~30 nm) layer was added due to its good stability against hydrogen plasma exposure. It was also reported that a high crystal quality of ITO films could be achieved by employing AZO as a buffer layer [24,31,32]. As-deposited ITO:Zr films showed a sheet resistance of 10.27 Ω/□, while sheet resistance varied from 12.84 to 10.68 Ω/□ with the increase of glass etching time from 30 to 75 min, respectively. On the other hand, the as-deposited ITO:Zr/AZO films showed a sheet resistance of 9.784 Ω/□, while sheet resistance varied from 10.96 to 9.335 Ω/□ with the increase of glass etching time from 30 to 75 min. Here, the minor variation of the sheet resistance may be related to the step coverage that was changed with the variation of

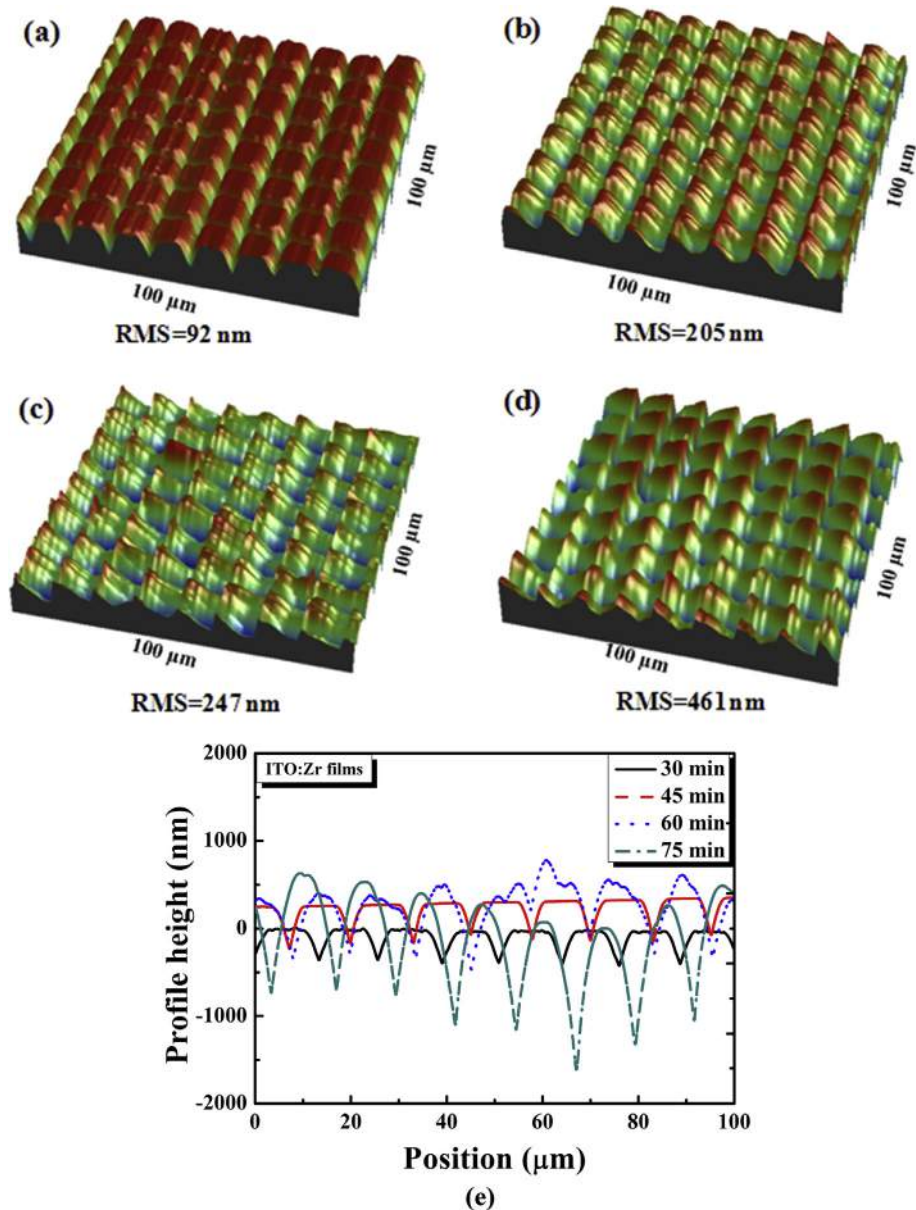


Fig. 4. 3-D alpha step profiler images of ITO:Zr films deposited on SF₆/Ar plasma textured glass surface morphologies for various etching times, of (a) 30 min, (b) 45 min, (c) 60 min, and (d) 75 min. (e) The profile height of ITO:Zr films as a function of glass etching time.

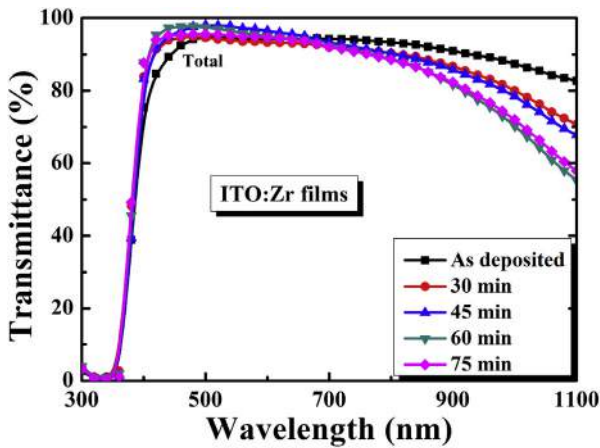
the surface morphology of TCO films [11,29,30]. The lowest sheet resistance is shown for the ITO:Zr and ITO:Zr/AZO films, with the glass etching time of 75 min Fig. 6(b) shows the electrical properties (i.e., resistivity, carrier concentration, and Hall mobility) of ITO:Zr/AZO films, as a function of glass etching time. As-deposited ITO:Zr/AZO films showed a resistivity of $2.182 \times 10^{-4} \Omega \text{ cm}$, whereas resistivity decreased from 2.818×10^{-4} to $1.632 \times 10^{-4} \Omega \text{ cm}$, with an increase of glass etching time from 30 to 75 min. The Hall mobility was shown as $27.06 \text{ cm}^2/\text{V}\cdot\text{s}$ for the as-deposited ITO:Zr/AZO films, while Hall mobility increased from 15.66 to $27.09 \text{ cm}^2/\text{V}\cdot\text{s}$ with the increase of glass etching time from 30 to 75 min. From the sheet resistance and electrical properties of ITO:Zr/AZO films, we can conclude that minor variation in the electrical properties was observed, due to the various step coverages [12,29,30]. Our textured glass ITO:Zr films showed the higher haze ratio, compared to the conventional FTO glass. Therefore, the ITO:Zr films with high transmittance, high rms roughness, and high haze ratio are considered very useful for the improvement of performance in a-Si TFSCs.

Fig. 7 shows the current density-voltage (J-V) characteristics of the a-Si TFSCs on flat and textured glass substrates, and Table 1 summarizes the results. The a-Si TFSCs deposited on flat glass substrates showed the short circuit current density (J_{SC}) and

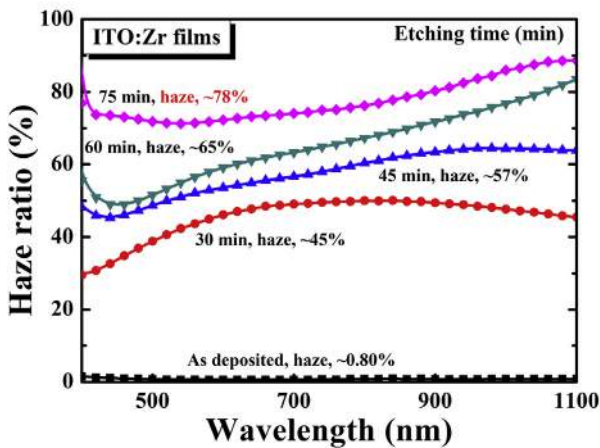
efficiency (η) of $10.52 \text{ mA}/\text{cm}^2$ and 5.88% , respectively [33–35]. The a-Si TFSCs deposited on textured glass with etching time of 30 min showed the J_{SC} and η of $10.60 \text{ mA}/\text{cm}^2$ and 6.05% , respectively. There was an increase in the J_{SC} of the device with higher etching time, without any change in FF or V_{oc} . The maximum performance of the a-Si TFSCs was shown as; $V_{oc} = 875 \text{ mV}$, $J_{SC} = 11.31 \text{ mA}/\text{cm}^2$, $FF = 70.90\%$, and $\eta = 7.02\%$, deposited on textured glass for the etching time of 75 min. Even though the performance of the a-Si TFSCs is not as high as that of the commercially available cell performance, we are hopeful to improve the J_{SC} and η of a-Si TFSCs by further investigations and overcoming the current issues [15,25]. Therefore, the textured glass ITO:Zr/AZO films with high transmittance, high haze ratio, and low sheet resistance can be employed for high efficiency a-Si TFSCs.

4. Conclusion

We report various SF_6/Ar plasma textured glass surface morphologies of high transmittance, haze ratio, and low sheet resistance ITO:Zr films for a-Si TFSCs. Due to micro- and nano-size textured features of SF_6/Ar plasma glass surface morphologies, the light can be scattered in visible and NIR wavelength regions. Various types of glass surface morphologies were observed via SF_6/Ar plasma texturing for the etching time from 30 to 75 min. The RF sputtered ITO:Zr films deposited on the textured glass surface morphologies showed the lowest sheet resistance of $10.68 \Omega/\square$, the highest total visible-NIR transmittance of 88.48% , and a high

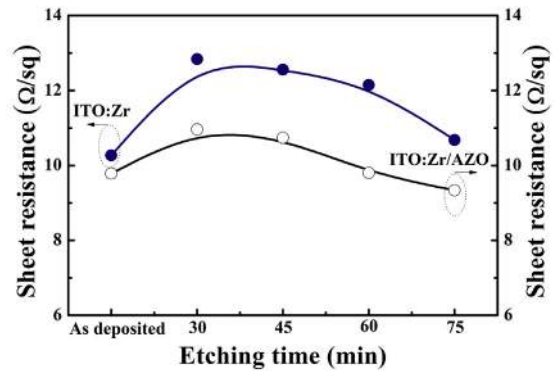


(a)

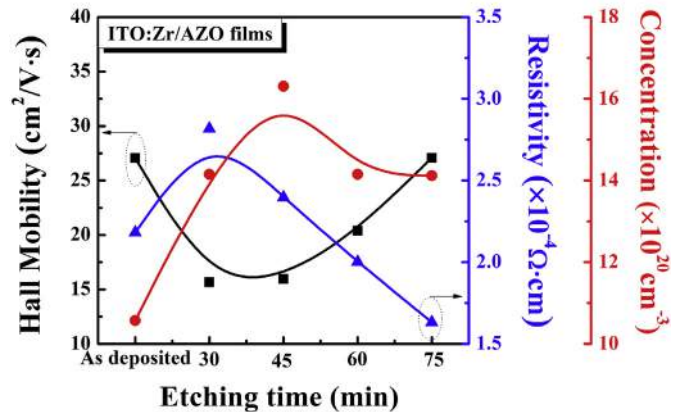


(b)

Fig. 5. The optical characteristics (a) total transmittance, and (b) Haze ratio of ITO:Zr films deposited on textured glass surface morphologies as a function of etching time.



(a)



(b)

Fig. 6. The sheet resistance of (a) ITO:Zr and ITO:Zr/AZO films, (b) the resistivity, Hall mobility and carrier concentration of ITO:Zr/AZO films deposited on SF_6/Ar plasma textured glass substrates, for various etching times.

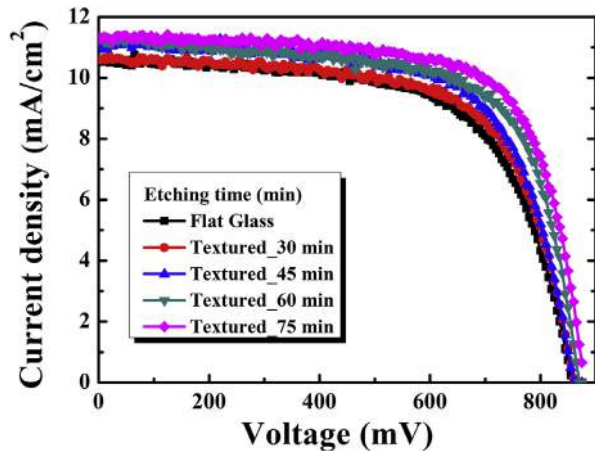


Fig. 7. The performance of amorphous silicon thin film solar cell, as a function of glass etching time.

Table 1

The performance of amorphous silicon thin film solar cells as a function of etching time.

Sample#	Etching time (min)	V_{OC} (mV)	J_{SC} (mA/cm ²)	FF (%)	η (%)
1	Flat Glass	855	10.52	65.36	5.88
2	30	860	10.60	66.33	6.05
3	45	860	11.06	67.19	6.39
4	60	865	11.29	69.06	6.73
5	75	875	11.31	70.90	7.02

haze ratio of 77.66%, in the visible-NIR wavelength region. The enhancement in haze ratio with an increase of etching time was related to the high rms roughness of the ITO:Zr films. It was also noted that the glass surface morphology has a minor influence on the sheet resistance and electrical characteristics of the ITO:Zr films that may be related to the step coverage. A thin AZO (~30 nm) layer was used as a passivation layer due to the good stability against hydrogen plasma exposure. The change of glass surface morphology did not influence the crystallinity of the ITO:Zr films. The textured glass ITO:Zr/AZO films were employed as a front electrode for the fabrication of a-Si TFSCs, and showed the J_{SC} and η of 11.31 mA/cm² and 7.02%, respectively.

Acknowledgments

This work was supported by the New & Renewable Energy Technology Development Program of the Korea Institute of Energy Technology Evaluation and Planning (KETEP) grant funded by the Korea government Ministry of Trade, Industry & Energy. (No.20143020010860).

References

- [1] Tan H, Psoadaki E, Isabella O, Fischer M, Babal P, Vasudevan R, et al. *Appl Phys Lett* 2013;103:173905–8.
- [2] Jovanov V, Palanchoke U, Magnus P, Stiebig H, Hüpkes J, Sichanugrist P, et al. *Opt Express* 2013;21:A595–606.
- [3] Zeman M, Isabella O, Jäger K, Santbergen R, Soltsev S, Topic M, et al. *Energy Procedia* 2012;15:189–99.
- [4] Isabella O, Krc J, Zeman M. *Appl Phys Lett* 2010;97:101106–8.
- [5] Hussain SQ, Ahn S, Park H, Kwon G, Raja J, Lee Y, et al. *Vacuum* 2013;94:87–91.
- [6] Hongsingthong A, Krajangsang T, Yunaz IA, Miyajima S, Konagai M. *Appl Phys Express* 2010;3:051102–5.
- [7] Hongsingthong A, Krajangsang T, Limmanee A, Sriprapha K, Sritharathikhun J, Konagai M. *Thin Solid Films* 2013;537:291–5.
- [8] Hongsingthong A, Krajangsang T, Jantong B, Sichanugrist P, Konagai M. In: *Photovoltaic specialists conference (PVSC)*, 37th IEEE; 2011. p. 000791–4.
- [9] Sai H, Koida T, Matsui T, Yoshida I, Saito K, Kondo M. *Appl Phys Express* 2013;6:104101–4.
- [10] Sahraei N, Venkataraj S, Aberle AG, Peters IM. *Energy Procedia* 2013;33:166–72.
- [11] Jantong B, Moriya Y, Hongsingthong A, Sichanugrist P, Konagai M. *Sol Energy Mater Sol Cells* 2013;119:209–13.
- [12] Jovanov V, Xu X, Shrestha S, Schulte M, Hüpkes J, Zeman M, et al. *Sol Energy Mater Sol Cells* 2013;112:182–9.
- [13] Tamang A, Hongsingthong A, Sichanugrist P, Jovanov V, Konagai M, Knipp D. *IEEE J Photovoltaics* 2014;4:16–21.
- [14] Feltrin A, Meguro T, Van Assche E, Suezaki T, Ichikawa M, Kuchiyama T, et al. *Sol Energy Mater Sol Cells* 2013;119:219–27.
- [15] Battaglia C, Hsu C-M, Söderström K, Escarré J, Haug F-J, Charrière M, et al. *ACS Nano* 2012;6:2790–7.
- [16] Li X, Abe T, Esashi M. *Sens Actuators A* 2001;87:139–45.
- [17] Lallement L, Rhallabi A, Cardinaud C, Peignon Fernandez MC. *J Vac Sci Technol A* 2011;29:051304–12.
- [18] Park JH, Lee NE, Lee J, Park JS, Park HD. *Microelectron Eng* 2005;82:119–28.
- [19] Hussain SQ, Kim S, Ahn S, Balaji N, Lee Y, Lee JH, et al. *Sol Energy Mater Sol Cells* 2014;122:130–5.
- [20] Hussain SQ, Kim S, Ahn S, Park H, Le A, Lee S, et al. *Met Mater Int* 2014;20:565–9.
- [21] Zhang B, Dong X, Xu X, Zhao P, Wu J. *Sol Energy Mater Sol Cells* 2008;92:1224–9.
- [22] Gessert TA, Burst J, Li X, Scott M, Coutts TJ. *Thin Solid Films* 2011;519:7146–8.
- [23] Yen WT, Lin YC, Ke JH. *Appl Surf Sci* 2010;257:960–8.
- [24] Addonizio ML, Spadoni A, Antonaia A. *Appl Surf Sci* 2013;287:311–7.
- [25] Banca J, Aswin H, Yuki M, Porponth S, Christophe RW, Makoto K. *Jpn J Appl Phys* 2012;51. 10NB14–4.
- [26] Mizuhashi M, Gotoh Y, Adachi K. *Jpn J Appl Phys* 1998;27:2053–61.
- [27] Zhu H, Hüpkes J, Bunte E, Owen J, Huang SM. *Sol Energy Mater Sol Cells* 2011;95:964–8.
- [28] Wang FH, Yang CF, Lee YH. *Nanoscale Res Lett* 2014;9:97–103.
- [29] Kondo T, Sawada Y, Akiyama K, Funakubo H, Kiguchi T, Seki S, et al. *Thin Solid Films* 2008;516:5864–7.
- [30] Kondo T, Funakubo H, Akiyama K, Enta H, Seki Y, Wang MH, et al. *J Cryst Growth* 2009;311:642–6.
- [31] Wang C, Mao Y, Zeng X. *Appl Phys A* 2013;110:41–5.
- [32] Yang HH, Kim HW, So SY, Park GC, Lee J, Na KJ. *Trans Electr Electron. Mater* 2013;14:90–3.
- [33] Muller J, Rech B, Springer J, Vanecek M. *Sol Ener* 2004;77:917–30.
- [34] Lee YJ, Park H, Ju M, Kim Y, Park J, Vinh Ai D, et al. *Energy* 2014;66:20–4.
- [35] Park H, Lee J, Kim H, Kim D, Raja J, Yi J. *Appl Phys Lett* 2013;102:191602–4.
- [36] Raja J, Jang K, Hussain SQ, Chatterjee S, Velumani S, Balaji N, et al. *Appl Phys Lett* 2015;106:033501–4.
- [37] Hussain SQ, Yen C, Khan S, Kwon G, Kim S, Ahn S, et al. *Mater Sci Semicond Process* 2015 [in press].
- [38] Khan S, Hussain SQ, Hwang D, Velumani S, Lee H. *Mater Sci Semicond Process* 2015 [in press], <http://dx.doi.org/10.1016/j.mssp.2015.01.019>.